

中国激光

预热对选区激光熔化 316L 不锈钢力学性能的影响

解妙霞^{*}, 辛琪珂, 李焱鑫, Khan Muhammad Raza

西安建筑科技大学机电工程学院, 陕西 西安 710311

摘要 为了提升激光增材制造 316L 不锈钢的综合性能, 比较了室温、预热 100 °C 和 200 °C 三种条件下选区激光熔化(SLM) 316L 不锈钢试样的组织、拉伸性能、冲击韧性和疲劳性能。结果表明: SLM 制备的 316L 具有显著的各向异性。沿水平面方向和沿垂直方向取样时, 试样室温冲击功分别约为轧制板材的 47% 和 44%; 室温制备 SLM 试样承受垂直方向载荷时的抗拉强度约为其承受水平方向载荷时的抗拉强度的 81.6%。预热对致密度和冲击韧性的影响很小; 预热使显微硬度和抗拉强度略微降低、延伸率略微提高, 但总体上变化不显著。在所设置的试验条件下, 预热对试样承受垂直方向载荷时的疲劳寿命的影响很小, 但使试样承受水平方向载荷时的疲劳寿命得到明显提高。分析认为, 预热后试样在疲劳试验中需要经历更多循环载荷加载次数才能达到临界裂纹尺寸。

关键词 激光技术; 选区激光熔化; 预热温度; 力学性能; 各向异性

中图分类号 TG405

文献标志码 A

doi: 10.3788/CJL202249.0802016

1 引言

选区激光熔化(SLM)被认为是激光制造技术的巅峰, 它通过选择性熔化粉末层直接生成功能复杂的零件, 在制造具有复杂形状三维物体时具有独特优势。该技术在生物医学、航空航天、冶金等领域得到了广泛应用, 是国内外的研究热点^[1-8]。其中, 316L 不锈钢由于焊接性好、耐蚀性好、力学性能优良、延展性好而被广泛关注^[9-16]。

余晨帆等^[9]认为, 选区激光熔化技术制备的 316L 不锈钢的晶粒内部纳米尺度胞状结构有助于强度的提升, 同时拉伸过程中奥氏体晶粒内部产生形变孪晶, 因此具有较好的强塑性匹配。刘文杰等^[10]研究发现, 选区激光熔化成形 316L 不锈钢的组织和冲击韧性存在着明显的各向异性, 其中水平截面的晶粒细化, 大角度晶界数目多且韧性更好。周玥丞等^[11]采用不同设备、不同厚度和不同方向取样的方案开展了 SLM 制备 316L 不锈钢的力学性能及其各向性的比较研究。尹燕等^[12]基于“微熔池”散热条件特点, 分析了选区激光熔化成形 316L

不锈钢的微观组织及拉伸性能各向性的形成机理。曾寿金等^[13]研究了选区激光熔化成形 316L 不锈钢的不同多孔结构的力学性能, 对比分析了不同多孔结构与人骨的匹配性。杨鑫等^[14]针对细粉成本高的问题, 将 316L 细粉与粗粉混合, 研究表明, 在引入 20% (质量分数) 大颗粒粉末的条件下, 沉积态试样仍具有良好的相对密度和力学性能。黄明吉等^[15]研究了 SLM 成形 316L 工艺对滑动磨损特性及硬度的影响, 认为孔隙率与磨损量及硬度存在相关性: 孔隙率越小, 硬度越大, 磨损率越小。向召伟等^[16]建立了 SLM 成形 316L 不锈钢的多道扫描温度场数值模拟模型, 研究了选区激光熔化关键工艺参数对熔池稳定性和冷却速度的影响。

SLM 工艺的特点及其对疲劳性能的影响一直备受关注。在 SLM 过程中, 少量粉末迅速熔化随后迅速凝固, 在合金中形成分级的精细组织^[17]。SLM 合金中的微孔隙很难完全消除。SLM 合金逐层外延生长可能形成具有明显方向性的粗大柱状晶。Kumar 等^[18]分析了加工硬化对疲劳强度的影响, 认为 SLM 合金中细小的胞状晶使 SLM 合金承

收稿日期: 2021-08-31; 修回日期: 2021-10-16; 录用日期: 2021-10-21

基金项目: 国家重点研发计划(2018YFB1105800)、陕西省自然科学基金(2020JM484)

通信作者: *xiemiaoxia@xauat.edu.cn

受载荷时不发生加工硬化,导致SLM合金的疲劳强度降低,而粗大柱状晶具有明显的方向性,也会使SLM合金的疲劳强度降低。Wang等^[19]分析了应力状态对SLM合金疲劳强度的影响。

预热是简便易行的调控组织性能的手段,被用于开裂倾向大的模具钢、工具钢和铝合金等的SLM成形,可以有效减小残余应力、翘曲变形和局部开裂倾向^[20-26]。预热对选区激光熔化316L不锈钢力学性能的影响尚未受到太多关注,尤其是关于预热对选区激光熔化316L不锈钢疲劳性能的影响缺乏研究。本文系统比较了室温、预热100℃和200℃三种条件下选区激光熔化316L不锈钢的组织、显微

硬度、拉伸性能、冲击韧性和疲劳性能,旨在拓展提升激光增材制造316L不锈钢综合性能的可能途径。

2 试验材料及设备

2.1 试验材料

本文采用气雾化方法制备316L不锈钢粉末,其化学成分如表1所示。图1是扫描电镜(SEM)下观察到的316L不锈钢粉末的形貌及粒径分布,粉末粒径分布范围为15~53μm。试验前对粉末进行烘干和球磨处理。基板是厚度为10mm的316L不锈钢,试验前用乙醇清理基板表面。

表1 316L不锈钢粉末的化学成分

Table 1 Chemical compositions of 316L stainless steel powder

Element	Cr	Ni	Mo	Mn	Si	N	C	P	S	Fe
Mass fraction /%	17.360	11.080	2.020	1.190	0.360	0.520	0.013	0.032	0.002	Bal.

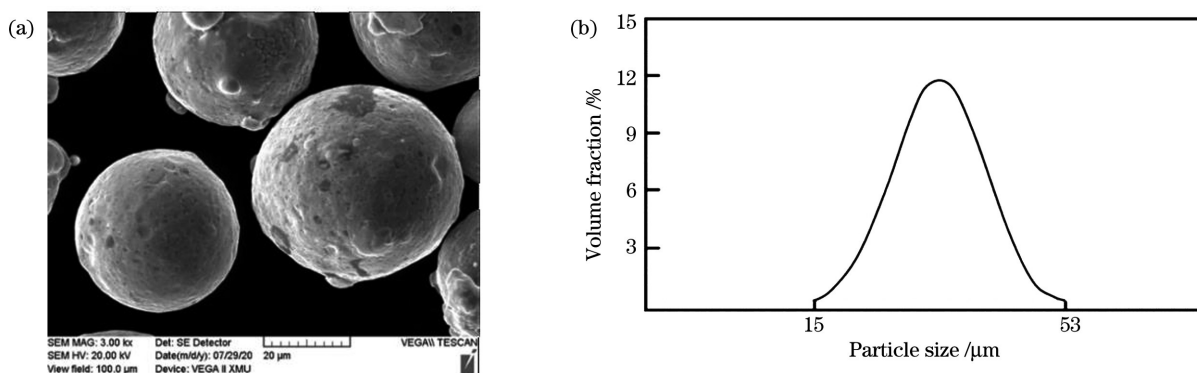


图1 316L不锈钢粉末。(a)微观形貌图;(b)粒径分布图

Fig. 1 316L stainless steel powder. (a) Microstructure; (b) particle size distribution

2.2 试验方法与设备

选区激光熔化成形试验采用西安交通大学的JG-SLM260设备完成。该设备采用单缸单向定量送粉系统,粉层厚度范围为0.02~0.10mm。该设备的激光源为IPG公司500W的单模连续光纤激光器,波长为1.07μm,焦斑直径为50μm,焦距为130mm,最大激光扫描速度为7000mm/s,最大成形尺寸为260mm×260mm×300mm,成形室保护气为氩气。SLM试验前对成形室进行清洗,确保试验中氧元素含量(体积分数)不超过0.1×10⁻⁶。SLM试验中激光扫描方式及x,y,z方向的定义如图2(a)所示,打印过程中激光扫描方向逐层偏转一个固定的角度,第n层的扫描方向与第n+1层的扫描方向的夹角为67°。

采用表2所示的SLM参数,分别在不预热、预热100℃、预热200℃条件下进行316L不锈钢的

SLM试验。尺寸为10mm×10mm×10mm的SLM试样用来观察金相组织。

采用阿基米德排水法测量试样的致密度。金相试样横截面经砂纸打磨、抛光和乙醇清洗后,用5g CuSO₄+20mL H₂O+20mL HCl试剂腐蚀10s,然后在Nikon MA200光学显微镜下观察试样的横截面金相组织。采用Qness半自动显微硬度计测量试样横截面上的维氏显微硬度,载荷为200g,保载时间为15s。测试路径沿厚度方向从试样底部一直测试到顶部,相邻测试点的间隔为0.5mm。

室温下进行拉伸试验和夏比冲击试验,拉伸试验中拉伸速率恒定为0.5mm/min。每个方向上的拉伸试验和夏比冲击试验都重复三遍。室温疲劳试验的加载应力在150~0MPa之间按照正弦波形周期性变化,加载频率为20Hz。分别沿水平方向

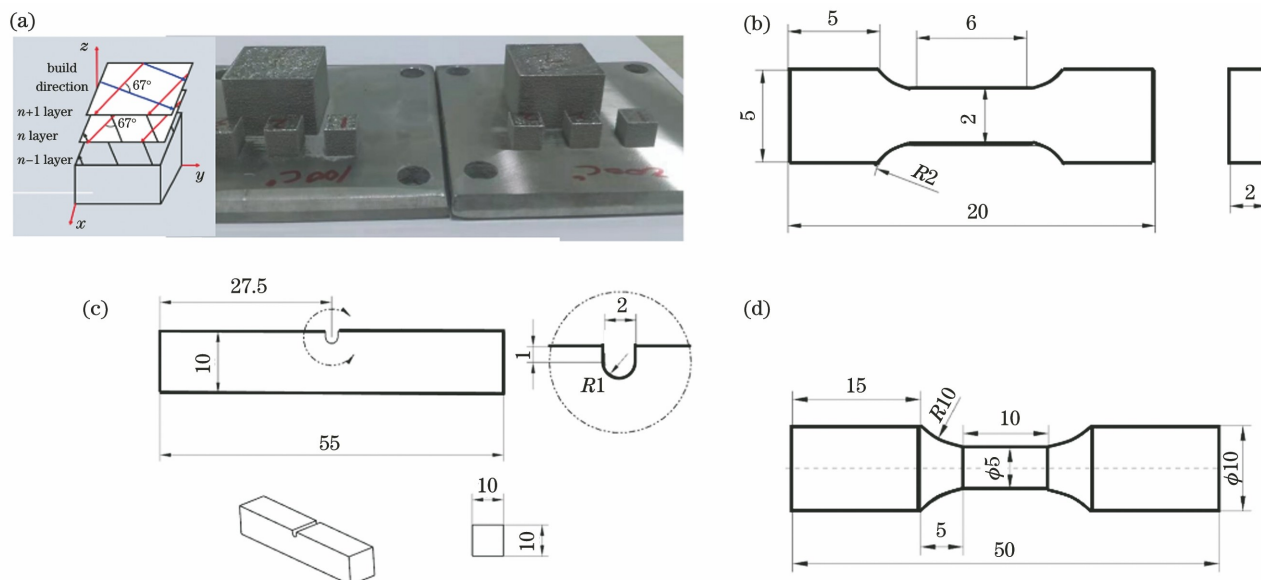


图 2 SLM 成形试样以及各试样的尺寸。(a) SLM 成形试样;(b)拉伸试样尺寸;(c)夏比冲击试样尺寸;(d)疲劳试样尺寸
Fig. 2 SLM formed samples and size drawings of various samples. (a) SLM formed samples; (b) dimensions of tensile specimens; (c) dimensions of impact specimens; (d) dimensions of fatigue specimens

表 2 以预热温度为变量的单因素试验

Table 2 Single factor test with preheating temperature as variable

Serial number	Laser power P / W	Scanning speed $v / (\text{mm} \cdot \text{s}^{-1})$	Scanning spacing h / mm	Layer thickness t / mm	Preheating temperature $T / ^\circ\text{C}$
1	400	900	0.05	0.03	Room temperature
2	400	900	0.05	0.03	100
3	400	900	0.05	0.03	200

($x-y$ 平面内) 和垂直方向 (z 向) 切取疲劳试样, 每个方向上的疲劳试验重复三遍。拉伸试样、夏比冲击试样和疲劳试样的尺寸如图 2 所示, 试样经过线切割而得到, 然后用相同牌号细砂纸打磨试样表面。采用 SEM 观察拉伸试样、夏比冲击试样和疲劳试样的断口显微形貌。

3 结果与讨论

3.1 预热对 316L-SLM 试样致密度的影响

比较了不同预热温度下 316L-SLM 试样的致密度, 如图 3 所示。可以看出, 预热温度为 100°C 时, 试样的致密度与室温下试样的致密度相同, 预热温度为 200°C 时, 试样的致密度比室温下试样的致密度高出 0.001。很显然, 对基板进行预热有利于 SLM 过程中金属粉末的熔化, 可能对试样致密度产生积极影响。不过, 从图 3 可以看出, 200°C 预热对致密度的积极影响是很小的。

3.2 预热温度对 316L-SLM 成形组织的影响

不同预热温度下试样截面的显微组织如图 4 所

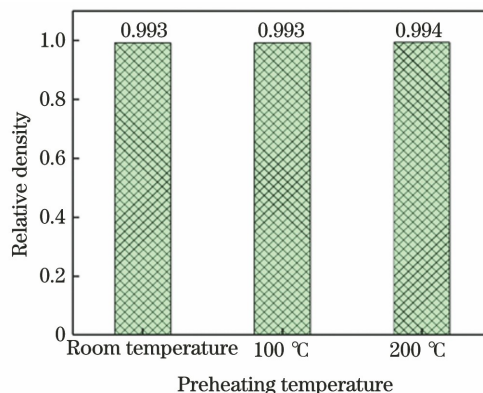


图 3 不同预热温度下 SLM 成形 316L 不锈钢试样的致密度

Fig. 3 Densities of 316L stainless steel samples formed by SLM under different preheating temperatures

示, 其中截面是沿着厚度方向上的截面, 即垂直截面。可以看出, 对于预热温度与室温下的试样截面, 鱼鳞状熔池均交替叠加, 这是由于采用了激光扫描方向逐层偏移 67° 的策略, 扫描方向与试样成形表面存在一定的角度。

预热条件下试样显微组织中的晶粒沿着层厚

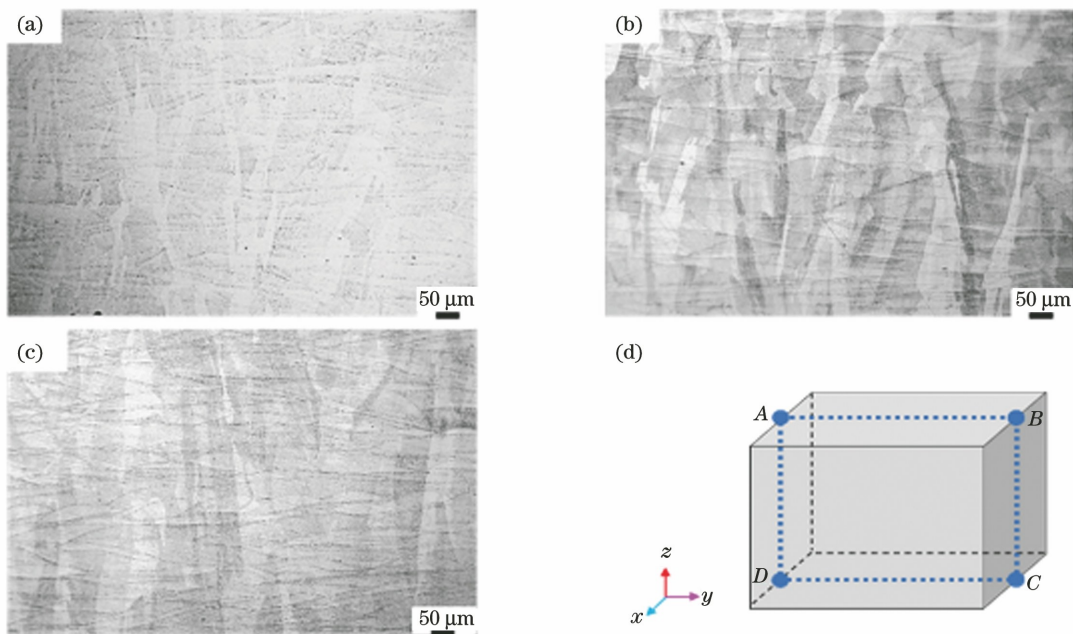


图4 不同预热温度下 SLM 试样的显微组织。(a)室温;(b)预热 100 °C;(c)预热 200 °C;(d)截面示意图

Fig. 4 Microstructures of SLM samples at different preheating temperatures. (a) Room temperature; (b) preheating at 100 °C; (c) preheating at 200 °C; (d) cross-sectional sketch

方向生长，并且穿过熔池的熔合线继续外延生长。由图4可以发现，经过两种温度预热后，晶粒尺寸的大小与室温下试样晶粒尺寸的大小没有明显的差异。

3.3 预热温度对316L-SLM试样横截面维氏硬度的影响

垂直截面上的维氏硬度测量结果如图5所示。轧制态316L钢(316L-R)的硬度平均值为292.6 HV。室温、预热100 °C和预热200 °C三个条件下SLM试样的硬度平均值分别为366.1, 350.5, 350.0 HV。结果表明，预热后316L-SLM成形件的维氏硬度略微减低，但两种不同预热温度下316L-SLM成形件的维氏硬度差别很小。

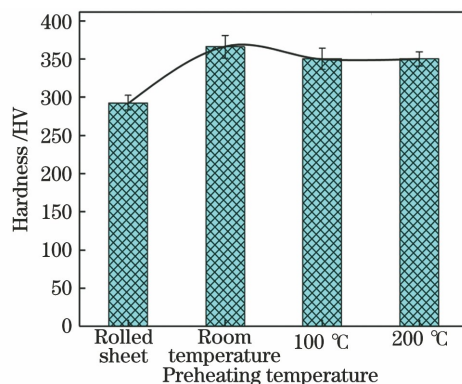


图5 不同预热温度下打印试样垂直截面上的平均硬度分布

Fig. 5 Average hardness distributions on vertical section of printed specimens at different preheating temperatures

3.4 预热温度对316L-SLM试样拉伸性能的影响

选区激光熔化成形试样不同方向上的力学性能呈现各向异性。本文SLM过程中的激光扫描方向逐层旋转，如图2(a)所示。因此，进行了水平方向和垂直方向两个拉伸试验。试验前用砂纸将拉伸试样表面打磨光滑，消除线切割痕迹及毛刺，避免应力集中现象。

图6(a)、(b)分别给出了不同预热温度下SLM成形316L试样沿水平方向和沿垂直方向的拉伸试验结果。为了比较，图6中给出了板材沿轧制方向的拉伸试验结果。

如图6(a)所示，轧制态板材的抗拉强度为739.12 MPa；沿水平方向加载时，室温、预热100 °C和预热200 °C三种条件下SLM试样的抗拉强度分别是816.58, 784.18, 789.78 MPa，三者均高于轧制态板材的抗拉强度。从图6(b)可见，沿垂直方向加载时，室温、预热100 °C和预热200 °C三种条件下SLM试样的抗拉强度分别是658.90, 625.28, 636.18 MPa，三者均低于轧制态板材的抗拉强度。可见预热后抗拉强度略有下降，但变化不显著。SLM成形316L试样的力学性能呈现各向异性，垂直方向的抗拉强度低于水平方向的抗拉强度，前者约为后者的80%。图6(a)、(b)结果还表明，SLM成形316L试样的延伸率远小于轧制态板材的延伸率，前者仅为后者的50%左右。相比室温下得到的

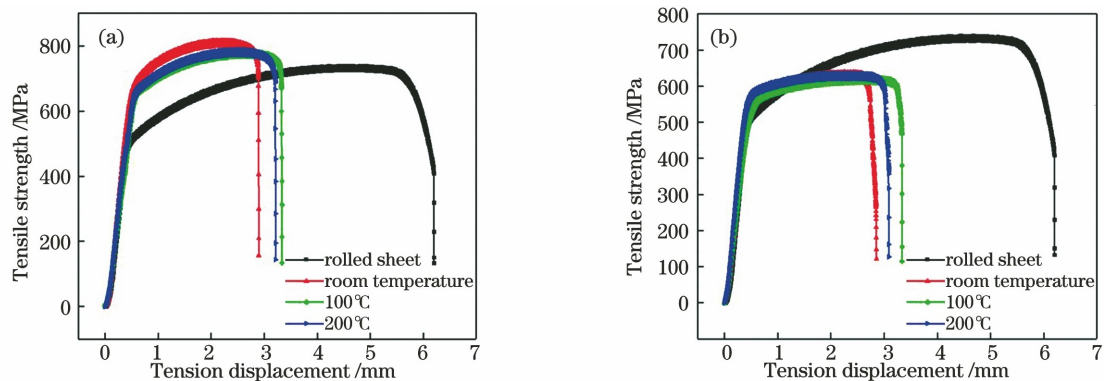


图 6 沿不同方向的拉伸结果。(a)沿水平方向;(b)沿垂直方向

Fig. 6 Tensile results in different directions. (a) Horizontal direction; (b) vertical direction

SLM 成形 316L 试样, 预热后 SLM 成形 316L 试样

在不同方向上的抗拉强度均略微降低、不同方向上的延伸率均略微提高。但总体上预热温度对打印试

样的强度和延伸率的影响都比较小。

图 7(a) 所示是轧制板材的拉伸断口形貌, 图 7(b)、(c)、(d) 分别是室温、预热 100 °C 和预热

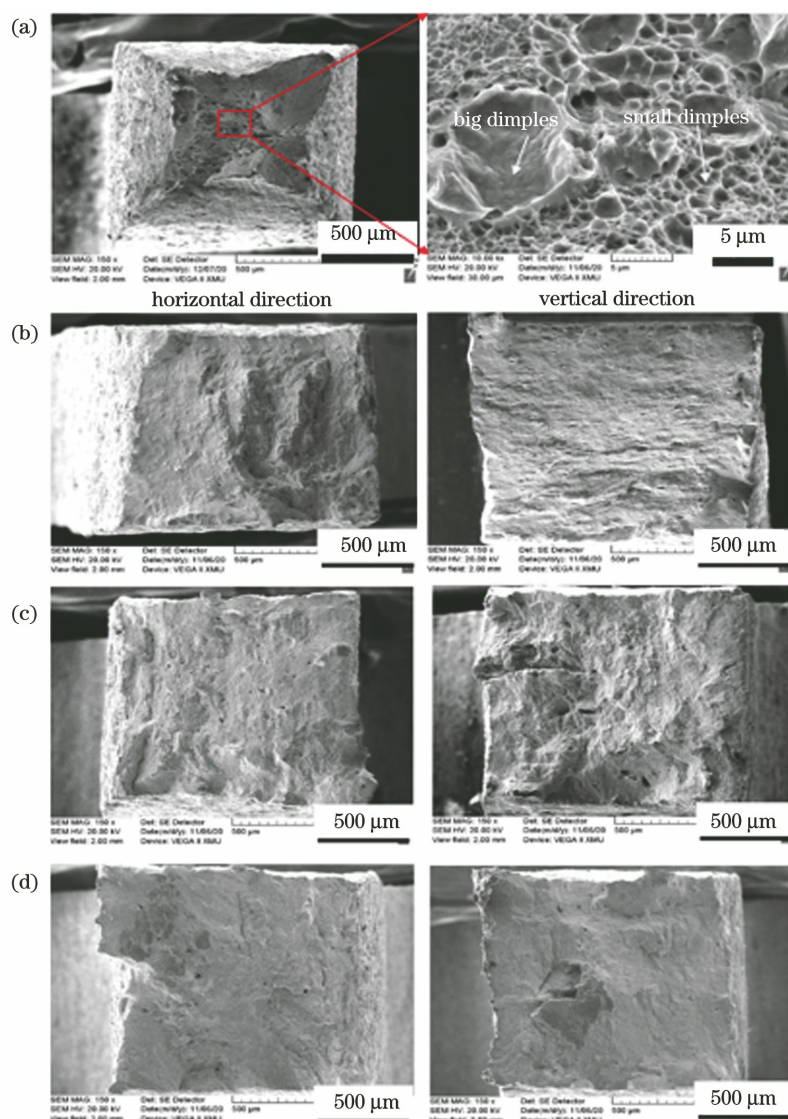


图 7 不同条件下拉伸断口的显微形貌。(a)轧制板材;(b)不预热;(c)预热 100 °C;(d)预热 200 °C

Fig. 7 Microstructures of tensile fractures under different conditions. (a) Rolled sheet; (b) no preheating; (c) preheating at 100 °C; (d) preheating at 200 °C

200 °C三种条件下 SLM 试样的拉伸断口形貌。

轧制板材断口的颈缩现象非常显著,断口布满了大尺寸韧窝,最大韧窝尺寸超过 5 μm。相比之下,SLM 试样拉伸断口的颈缩现象不明显,断口由韧窝、未熔合缺陷两种形貌组成,且韧窝尺寸比较小。比较 SLM 试样不同方向的断口形貌还可以看出,沿垂直方向拉伸断口上的未熔合缺陷比沿水平方向拉伸断口上的未熔合缺陷多。这可能是垂直方向抗拉强度低于水平方向抗拉强度的主要原因。

3.5 预热温度对 316L-SLM 试样室温冲击功的影响

图 8(a)、(b) 分别给出了不同预热温度下沿水平方向截取的 SLM 成形 316L 试样的室温冲击功和不同预热温度下沿垂直方向截取的 SLM 成形

316L 试样的室温冲击功。可以看出,热轧态 316L 不锈钢的室温冲击功为 146.69 J。沿水平方向取样时,室温、预热 100 °C 和预热 200 °C 三种条件下 SLM 试样的室温冲击功分别是 70.420, 71.005, 70.130 J, 三者数值相差不大,都约为热轧态 316L 不锈钢室温冲击功的 47%。沿垂直方向取样时,室温、预热 100 °C 和预热 200 °C 三种条件下 SLM 试样的室温冲击功分别是 63.125, 65.673, 65.165 J, 三者数值相差不显著,都约为热轧态 316L 不锈钢室温冲击功的 44%。总体上,SLM 试样的冲击功远小于轧制态试样的冲击功,SLM 试样沿垂直方向取样时的冲击功略小于沿水平方向取样时的冲击功,预热对 SLM 试样的冲击功影响很小。

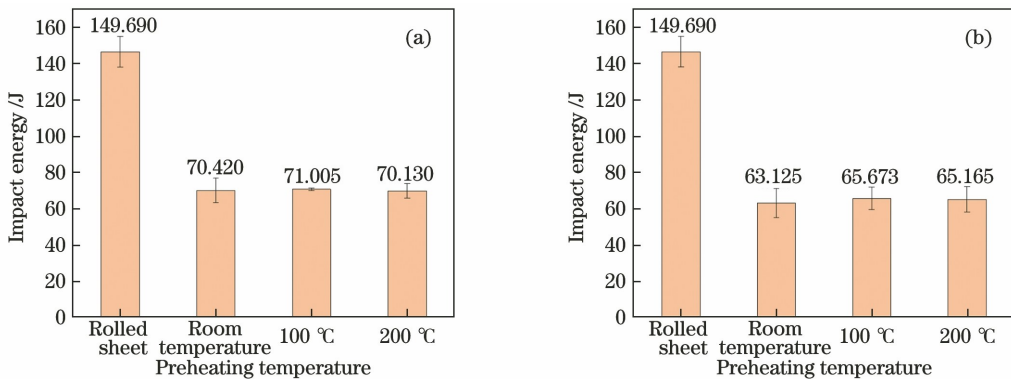


图 8 不同预热温度下试样的冲击功。(a)沿水平方向取样;(b)沿垂直方向取样

Fig. 8 Impact energy of specimens at different preheating temperatures. (a) Horizontal direction; (b) vertical direction

图 9(a) 所示为 316L-R 试样的冲击断口的显微

形貌,可以看到尺寸不均匀的大小韧窝。图 9(b)、

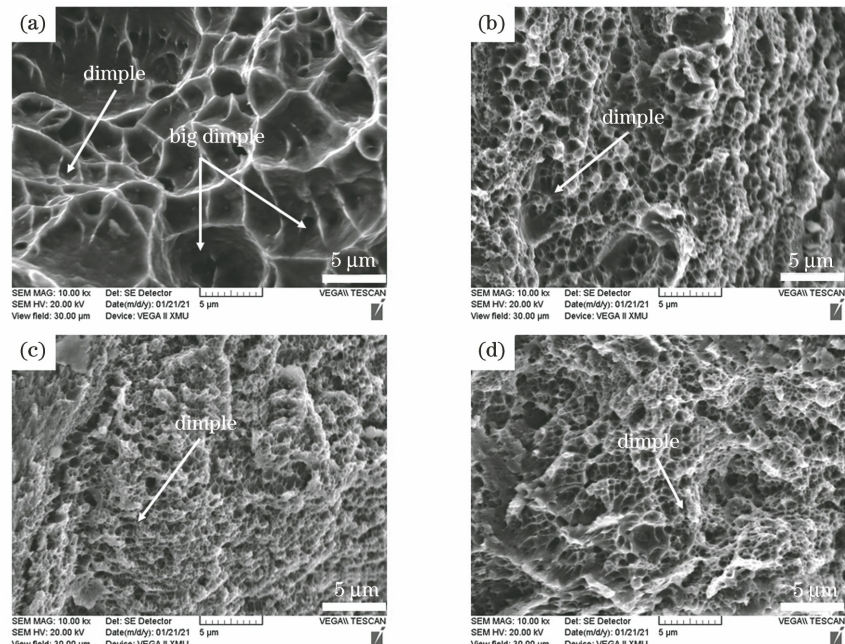


图 9 沿水平方向取样时不同条件下试样冲击断口的显微形貌。(a) 轧制态板材;

Fig. 9 Microstructures of impact fractures sampled along horizontal direction under different conditions. (a) Rolled sheet;

(b) room temperature; (c) preheating at 100 °C; (d) preheating at 200 °C

(c)、(d)分别为沿水平方向取样时室温、预热100℃和预热200℃三种条件下SLM试样的冲击断口的显微形貌。可以看到,三者断口显微形貌没有明显差异,断口中都分布着尺寸均匀的小韧窝,韧窝尺寸远小于轧制态板材断口的韧窝尺寸。

3.6 预热温度对316L-SLM试样抗疲劳性能的影响

图10(a)、(b)分别给出了沿水平方向加载时的疲劳试验结果和沿垂直方向加载时的疲劳试验结果。为了便于比较,轧制态316L的疲劳试验结果也在此给出。可以看出,轧制态316L的疲劳试样在循环次数达 2×10^6 时仍未发生断裂。

从图10(a)可以看出,沿水平方向加载时,室温、预热100℃和预热200℃三种条件下SLM试样发生疲劳断裂的循环次数分别是562890.3、

1446426、1478941。从图10(b)可以看出,沿垂直方向加载时,室温、预热100℃和预热200℃三种条件下SLM试样发生疲劳断裂的循环次数分别是236070、208394、218500。从图10可以看出,对于两个加载方向,同一加载方向上两种预热温度下所获SLM试样的疲劳寿命的差别不是很大。比较图10(a)和图10(b)可知,对于室温SLM试样,其承受垂直方向循环载荷时的疲劳寿命约为承受水平方向循环载荷时的疲劳寿命的42%。预热可以使SLM试样承受水平方向循环载荷的疲劳寿命大幅提高,其中预热100℃和预热200℃时SLM试样承受水平方向循环载荷的循环次数分别约为室温SLM试样的2.58倍和2.64倍。但是,预热对SLM试样承受垂直方向循环载荷的疲劳寿命的影响很小。

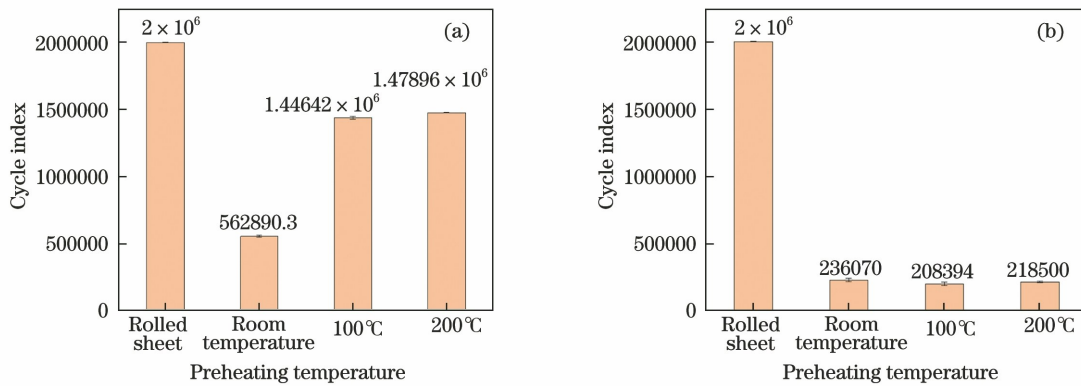


图10 不同预热温度下试样的疲劳寿命。(a) 沿水平方向加载;(b)沿垂直方向加载

Fig. 10 Fatigue life of specimens at different preheating temperatures. (a) Loaded along horizontal direction;
(b) loaded along vertical direction

图11显示了疲劳试验后试样断口形貌。图11(a)、(b)、(c)分别是在水平方向载荷作用下室温、预热100℃及预热200℃时三种SLM试样的疲劳断口。图11(d)、(e)、(f)分别是在垂直方向载荷作用下室温、预热100℃及预热200℃时三种SLM试样的疲劳断口。疲劳失效过程分为三个主要阶段,即疲劳裂纹形成、疲劳裂纹扩展和最终的断裂。最终的断裂阶段对疲劳寿命的影响可以忽略。比较图11(a₂)、(c₂)中的疲劳辉纹间距,可清楚地看到,图11(c₂)中的疲劳辉纹间距明显大于图11(a₂)中的疲劳辉纹间距,而图11(c)中试样的疲劳寿命远高于图11(a)中试样的疲劳寿命。这说明各试样疲劳寿命的决定因素不是疲劳裂纹扩展阶段,而是疲劳裂纹形成阶段。换句话说,与不预热试样相比,当预热试样承受水平方向载荷时,要达到临界裂纹尺寸,需要经历更多的载荷循环次数。根据线弹性断裂力学理论,利用基于大裂纹的临界应力强度因

子(ΔK_{th}^{LC}),可以计算出临界裂纹尺寸(a_c),当裂纹尺寸小于该数值时裂纹不扩展。临界裂纹尺寸^[27-28]的表达式为

$$a_c = \frac{1}{\pi} \left(\frac{\Delta K_{th}^{LC}}{Y \cdot \sigma_a} \right)^2, \quad (1)$$

式中: Y 为形状因子,可取值为1.1^[28];SLM316L的 ΔK_{th}^{LC} 值可取为9.1 MPa^[29];应力幅 σ_a 的数值为150 MPa。因此可以得到 $a_c = 968 \mu\text{m}$ 。可见图11中各试样疲劳裂纹起裂处的缺陷尺寸远小于临界裂纹尺寸 a_c 。

材料中的疲劳裂纹萌生取决于许多因素,其中一个重要因素是位错与微观结构元素(如晶界、夹杂物和气孔^[30])的相互作用。孔隙材料的疲劳寿命往往低于无孔隙材料。SLM成形316L中有大量孔洞缺陷,SLM小熔池快速冷却形成的精细胞状结构促使位错在塑性变形刚开始时就发生交叉滑移,几乎没有加工硬化阶段^[29]。在SLM合金中,可显著提

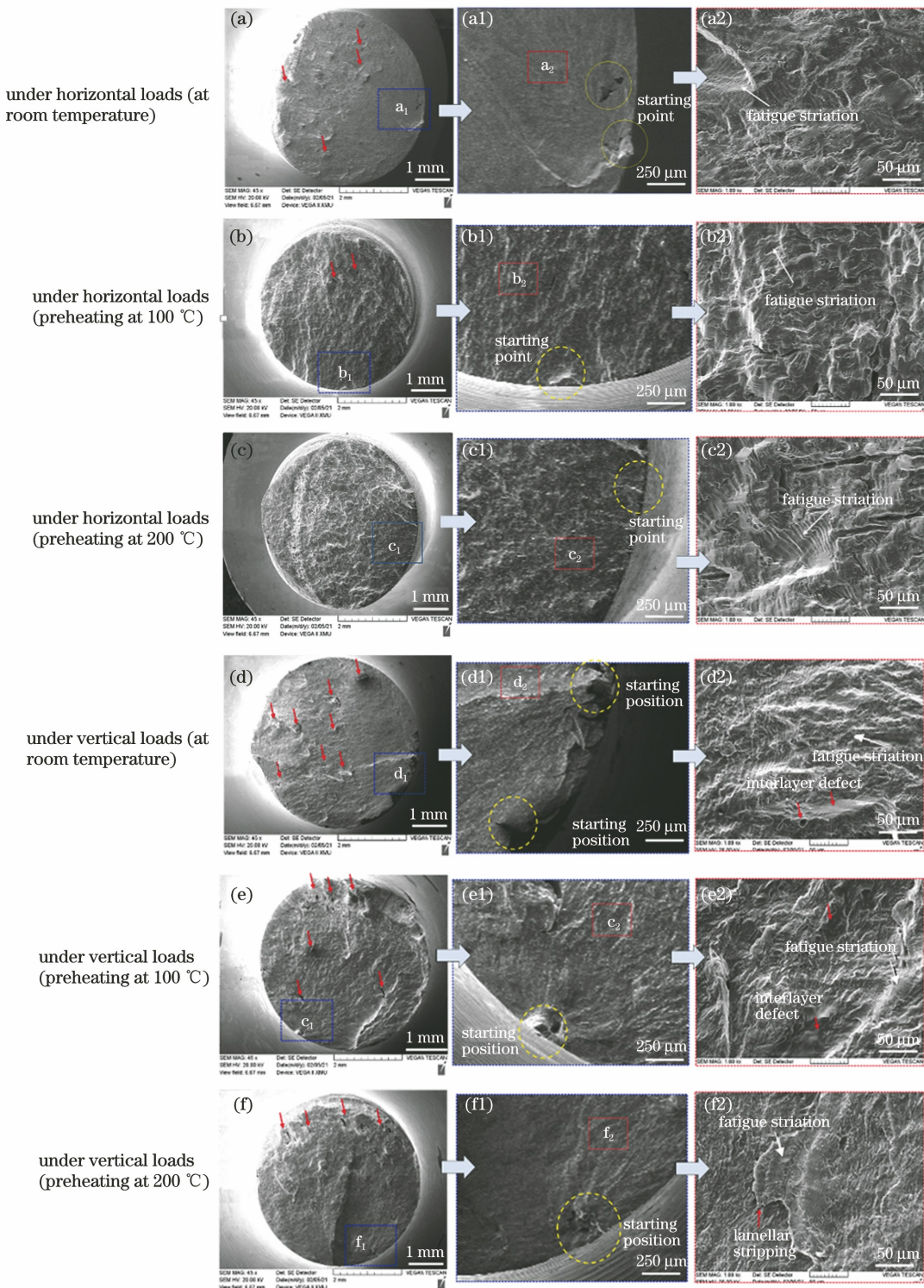


图 11 不同预热温度下试样的疲劳断口形貌

Fig. 11 Fatigue fracture morphologies of specimen under different preheating temperatures

高屈服强度的胞状组织过于细小,而柱状晶粒粗大且具有明显的方向性,这都不利于裂纹扩展方向的偏转和裂纹扩展的停止^[18]。SLM 试样中一半柱状晶界的取向偏差小于 5°,晶界对阻止疲劳裂纹的扩展也不太有效^[18],这些都会导致疲劳寿命下降。因

此 SLM 成形 316L 的疲劳寿命远小于轧制态 316L 的疲劳寿命。尤其是当载荷方向与层间界面垂直时,层间熔合不良缺陷的存在会使裂纹扩展更快^[18],因此 SLM 成形 316L 承受垂直方向循环载荷时的疲劳寿命远低于承受水平方向循环载荷时的疲

劳寿命。

4 结 论

对室温、预热100℃和预热200℃三种条件下SLM成形的316L不锈钢进行了显微组织和力学性能评价，并与316L不锈钢常规轧制板材进行了对比，得到如下结论。

1) 预热能使致密度略微提高，使维氏显微硬度的平均值减小4%左右。

2) SLM成形316L试样的延伸率约为轧制态板材延伸率的50%，承受垂直方向加载时其抗拉强度约为承受水平方向加载时的80%。预热后SLM成形316L试样不同方向的延伸率均可提高约6%；不同方向的抗拉强度均降低了4%左右，但仍然大于轧制板材的抗拉强度。

3) 预热对SLM试样的室温冲击功的影响不大，沿水平方向取样时SLM试样的室温冲击功约为热轧态316L不锈钢室温冲击功的47%，沿垂直方向取样时SLM试样的室温冲击功约为热轧态316L不锈钢室温冲击功的44%。

4) 室温制备的SLM试样承受垂直方向循环载荷时的疲劳寿命约为承受水平方向循环载荷时疲劳寿命的42%。预热对SLM试样承受垂直方向循环载荷时的疲劳寿命的影响很小，使SLM试样承受水平方向循环载荷时的疲劳寿命明显增大。分析认为，与不预热试样相比，要达到临界裂纹尺寸，预热试样需要经历更多的载荷循环次数。

参 考 文 献

- [1] Luo X P, Wei Y X, Huang H N, et al. Study on the precision of fabrication of dental pure titanium long-span scaffolds by selective laser melting[J]. Chinese Journal of Stomatology, 2021, 56(7): 646-651.
- [2] Hu Y B, Huang X N, Ding S B. Research progress of laser selective melting for outer space light weight drilling tools[J]. Mechanical Engineering and Technology, 2021, 10(1): 11.
- [3] 胡宇博, 黄西娜, 丁首斌. 激光选区熔化制备外太空轻质钻具的研究进展[J]. 机械工程与技术, 2021, 10(1): 11.
- [4] Zhao X, He K T, Li H X. Microstructure of selective laser melting parts under different scanning strategies[J]. Aeronautical Manufacturing Technology, 2019, 62(Z1): 64-71.
- [5] Ouyang H, He K T, Li H X, et al. Effects of scanning strategies on microstructure and properties of 316L stainless steel produced by selective laser melting[J]. Materials Science and Engineering of Powder Metallurgy, 2019, 24(1): 15-20.
- [6] Niu P D, Li R D, Yuan T C, et al. Effects of selective laser melting energy density on density and microstructure and properties of pure tungsten[J]. Materials Science and Engineering of Powder Metallurgy, 2019, 24(1): 15-20.
- [7] 牛朋达, 李瑞迪, 袁铁锤, 等. 能量密度对选区激光熔化纯钨致密度及组织性能的影响[J]. 粉末冶金材料科学与工程, 2019, 24(1): 15-20.
- [8] Wu M L, Sun H T, Sun X K, et al. Effect of process parameters on the deformation of selective laser melting[J]. Laser & Optoelectronics Progress, 2020, 57(5): 051403.
- [9] 吴懋亮, 孙翰霆, 孙玄锴, 等. 工艺参数对选区激光熔化中成形形变的影响[J]. 激光与光电子学进展, 2020, 57(5): 051403.
- [10] Zhang J Q, Wang M J, Liu J Y, et al. Influence of defocusing distance on microstructure and mechanical properties of 3D-printed 18Ni-300 maraging steel[J]. Chinese Journal of Lasers, 2020, 47(5): 0502004.
- [11] 张佳琪, 王敏杰, 刘建业, 等. 离焦量对3D打印18Ni-300马氏体时效钢组织和力学性能的影响[J]. 中国激光, 2020, 47(5): 0502004.
- [12] Gu D D, Zhang H M, Chen H Y, et al. Laser additive manufacturing of high-performance metallic aerospace components[J]. Chinese Journal of Lasers, 2020, 47(5): 0500002.
- [13] 顾冬冬, 张红梅, 陈洪宇, 等. 航空航天高性能金属材料构件激光增材制造[J]. 中国激光, 2020, 47(5): 0500002.
- [14] Yang C, Dong Z H, Chi C T, et al. Microstructure and mechanical properties of 24CrNiMo alloy steel formed by selective laser melting[J]. Chinese Journal of Lasers, 2020, 47(5): 0502008.
- [15] 杨晨, 董志宏, 迟长泰, 等. 选区激光熔化成形24CrNiMo合金钢的组织结构与力学性能[J]. 中国激光, 2020, 47(5): 0502008.
- [16] Yu C F, Zhao C C, Zhang Z F, et al. Tensile properties of selective laser melted 316L stainless steel[J]. Acta Metallurgica Sinica, 2020, 56(5): 683-692.
- [17] 余晨帆, 赵聪聪, 张哲峰, 等. 选区激光熔化316L不锈钢的拉伸性能[J]. 金属学报, 2020, 56(5): 683-692.
- [18] Zong X W, Liu W J, Yang Y M, et al. Anisotropy in microstructure and impact toughness of 316L austenitic stainless steel produced by selective laser melting[J]. Rare Metal Materials and Engineering, 2020, 56(5): 683-692.

- 2020, 49(12): 4031-4040.
- 宗学文, 刘文杰, 杨雨蒙, 等. 激光选区熔化316L奥氏体不锈钢微观组织和冲击韧性的各向异性研究[J]. 稀有金属材料与工程, 2020, 49(12): 4031-4040.
- [11] Zhou Y C, Zhao Y. Tensile performance of 316L stainless steel by additive manufacturing[J]. China Civil Engineering Journal, 2020, 53(10): 26-35.
- 周玥丞, 赵阳. 增材制造技术制备316L不锈钢的拉伸性能[J]. 土木工程学报, 2020, 53(10): 26-35.
- [12] Yin Y, Liu P Y, Lu C, et al. Microstructure and tensile properties of selective laser melting forming 316L stainless steel[J]. Transactions of the China Welding Institution, 2018, 39(8): 77-81, 132-133.
- 尹燕, 刘鹏宇, 路超, 等. 选区激光熔化成形316L不锈钢微观组织及拉伸性能分析[J]. 焊接学报, 2018, 39(8): 77-81, 132-133.
- [13] Zeng S J, Wu Q R, Ye J H. Mechanical properties of 316L stainless steel porous structure formed by selective laser melting[J]. Infrared and Laser Engineering, 2020, 49(8): 20190523.
- 曾寿金, 吴启锐, 叶建华. 选区激光熔化成型316L不锈钢多孔结构的力学性能[J]. 红外与激光工程, 2020, 49(8): 20190523.
- [14] Yang X, Ren Y J, Liu S F, et al. Microstructure and tensile property of SLM 316L stainless steel manufactured with fine and coarse powder mixtures [J]. Journal of Central South University, 2020, 27(2): 334-343.
- 杨鑫, 任垚嘉, 刘世锋, 等. 混合粉末制备沉积态316L不锈钢的组织和性能[J]. 中南大学学报, 2020, 27(2): 334-343.
- [15] Huang M J, Yang Y C, Feng S C. Effect of 316L SLM forming process on sliding wear characteristics and hardness[J]. Surface Technology, 2020, 49(1): 221-227.
- 黄明吉, 杨颖超, 冯少川. SLM成形316L工艺对滑动磨损特性及硬度的影响[J]. 表面技术, 2020, 49(1): 221-227.
- [16] Xiang Z W, Yin M, Yin G F, et al. Influence of critical process parameters on the thermal physical process in selective laser melting[J]. Advanced Engineering Sciences, 2020, 52(1): 134-142.
- 向召伟, 殷鸣, 殷国富, 等. 激光选区熔化关键工艺参数对热物理过程的影响[J]. 工程科学与技术, 2020, 52(1): 134-142.
- [17] Wang Y M, Voisin T, McKeown J T, et al. Additively manufactured hierarchical stainless steels with high strength and ductility[J]. Nature Materials, 2018, 17(1): 63-71.
- [18] Kumar P, Jayaraj R, Suryawanshi J, et al. Fatigue strength of additively manufactured 316L austenitic stainless steel[J]. Acta Materialia, 2020, 199: 225-239.
- [19] Wang Y Y, Su Z L. Effect of micro-defects on fatigue lifetime of additive manufactured 316L stainless steel under multiaxial loading[J]. Theoretical and Applied Fracture Mechanics, 2021, 111: 102849.
- [20] Liu Y, Wang M J, Qi W J, et al. Simulation analysis of cracking for 3D printed stainless steel mold molding parts[J]. Die & Mould Manufacture, 2021, 21(5): 61-69.
- 刘煜, 王敏杰, 戚文军, 等. 3D打印不锈钢模具成型零件开裂的模拟分析研究[J]. 模具制造, 2021, 21(5): 61-69.
- [21] Mertens R, Vrancken B, Holmstock N, et al. Influence of powder bed preheating on microstructure and mechanical properties of H13 tool steel SLM parts[J]. Physics Procedia, 2016, 83: 882-890.
- [22] Kempen K, Vrancken B, Buls S, et al. Selective laser melting of crack-free high density M2 high speed steel parts by baseplate preheating[J]. Journal of Manufacturing Science and Engineering, 2014, 136(6): 061026.
- [23] Sander J, Hufenbach J, Giebel L, et al. Microstructure and properties of FeCrMoVC tool steel produced by selective laser melting[J]. Materials & Design, 2016, 89: 335-341.
- [24] Ali H, Ma L, Ghadbeigi H, et al. *In-situ* residual stress reduction, martensitic decomposition and mechanical properties enhancement through high temperature powder bed pre-heating of selective laser melted Ti₆Al₄V[J]. Materials Science and Engineering: A, 2017, 695: 211-220.
- [25] Uddin S Z, Murr L E, Terrazas C A, et al. Processing and characterization of crack-free aluminum 6061 using high-temperature heating in laser powder bed fusion additive manufacturing[J]. Additive Manufacturing, 2018, 22: 405-415.
- [26] Wang W, Xie Z J, Zhao Z Y, et al. Influence of scanning path on the temperature field in selective laser melting[J]. Laser & Optoelectronics Progress, 2020, 57(5): 051401.
- 王稳, 谢志江, 赵增亚, 等. 扫描路径对选区激光熔化温度场的影响[J]. 激光与光电子学进展, 2020, 57(5): 051401.
- [27] El Haddad M H, Topper T H, Smith K N. Prediction of non propagating cracks[J]. Engineering Fracture Mechanics, 1979, 11(3): 573-584.
- [28] Kumar P, Ramamurty U. High cycle fatigue in selective laser melted Ti-6Al-4V[J]. Acta Materialia, 2020, 194: 305-320.

- [29] Suryawanshi J, Prashanth K G, Ramamurty U. Mechanical behavior of selective laser melted 316L stainless steel[J]. Materials Science and Engineering: A, 2017, 696: 113-121.
- [30] Davidson D, Chan K, McClung R, et al. Small fatigue cracks[M]//Milne I, Ritchie R O, Karihaloo B. Comprehensive structural integrity. Amsterdam: Elsevier, 2003: 129-164.

Effect of Preheating on Mechanical Properties of 316L Stainless Steel Fabricated by Selective Laser Melting

Xie Miaoxia^{*}, Xin Qike, Li Yanxin, Khan Muhammad Raza

School of Mechanical and Electrical Engineering, Xi'an University of Architecture and Technology, Xi'an, Shaanxi 710311, China

Abstract

Objective The fundamental research of the selective laser melting (SLM) technology is a research hotspot at home and abroad. Because of its good weldability, corrosion resistance, mechanical properties, and ductility, 316L stainless steel has become one of the most widely concerned SLM materials. The characteristics of the SLM process and its negative effects on fatigue performance have been the bottleneck of popularization and application of the SLM technology. Preheating is a simple and easy method to control the microstructure and properties. It is used for SLM forming of die steel, tool steel, and aluminum alloy with a large cracking tendency, which can effectively reduce the residual stress, warping deformation, and local cracking tendency. However, the effect of preheating on the mechanical properties of the selective laser melted 316L stainless steel has not received much attention. In this paper, the microstructure, microhardness, tensile properties, impact toughness, and fatigue properties of the selected laser-melted 316L stainless steel at room temperature, preheated at 100 °C and 200 °C are systematically investigated in order to expand the possible ways for improving the comprehensive properties of 316L stainless steel manufactured by SLM.

Methods Using the JG-SLM260 selective laser melting equipment and the 316L stainless steel powder prepared by the gas atomization method, the SLM tests of 316L stainless steel are carried out under the conditions of no preheating, preheating at 100 °C and preheating at 200 °C, respectively. First, the relative density of the samples is measured by the Archimedes drainage method. Then, the cross-sectional microstructure is observed under the Nikon MA200 optical microscope. Vickers microhardness on the cross section of the sample is measured by the Qness semi-automatic microhardness tester with the load of 200 g and the load retention time of 15 s. The tensile test and the Charpy impact test are carried out at room temperature. In the tensile test, the tensile rate is 0.5 mm/min. The tensile test and the Charpy impact test are repeated three times in each direction. The room temperature fatigue tests are conducted by using Instron-1341, and the loading stress varies periodically in 150–0 MPa according to a sinusoidal waveform, and the loading frequency is 20 Hz. The fracture morphologies of the tensile specimen, the Charpy impact specimen, and the fatigue specimen are observed by the VEGA II XMU tungsten filament scanning electron microscope (SEM). In addition, the properties of the 316L stainless steel are compared between SLM and conventional rolling.

Results and Discussions It is found that preheating has little impact on the grain size. Preheating can increase the density slightly and reduce the average Vickers microhardness by about 4%. The relative density of the sample with a preheating temperature of 100 °C is the same as that of the sample prepared at room temperature, and the relative density of the sample with a preheating temperature of 200 °C is higher by just 0.1% than that of the sample prepared at room temperature. The average hardnesses of the SLM samples at room temperature, preheated at 100 °C and preheated at 200 °C are 366.1, 350.5, and 350.0 HV, respectively. The tensile strength of the rolled 316L sheet is 739.12 MPa. In the horizontal tensile direction, the tensile strengths of the SLM samples obtained at room temperature, preheated at 100 °C, and preheated at 200 °C are 816.58, 784.18, and 789.78 MPa, respectively. All of them are higher than the tensile strength of the rolled sheet. In the vertical tensile direction, the tensile strengths of SLM samples obtained at room temperature, preheated at 100 °C, and preheated at 200 °C are

658.9, 625.28, and 636.18 MPa, respectively. All of them are lower than the tensile strength of the rolled sheet. The tensile strength increases slightly by preheating, but not significantly. In addition, the elongation of the SLM-formed 316L sample is about 50% of that of the rolled sheet, and its tensile strength under vertical loading is about 80% of that under horizontal loading. After preheating, the elongation of the 316L sample formed by SLM in different directions increases by about 6%, and the tensile strength decreases by about 4%. Preheating has little effect on the impact absorbing energy of the SLM sample at room temperature. The impact absorbing energy of the SLM sample sampled horizontally at room temperature is about 47% of that of the hot-rolled 316L stainless steel, and that of the SLM sample sampled vertically is about 44% of that of the hot-rolled 316L stainless steel. When sampling in the horizontal direction, the numbers of cycles of the fatigue fracture of the SLM samples obtained at room temperature, preheated at 100 °C, and preheated at 200 °C are 560890, 1446426, and 1478941, respectively. When sampling in the vertical direction, the numbers of cycles of the fatigue fracture of the SLM samples obtained at room temperature, preheated at 100 °C, and preheated at 200 °C are 236070, 208394, and 218500, respectively. The fatigue life of the SLM samples prepared at room temperature under a vertical cyclic load is about 42% of that under a horizontal cyclic load. Preheating has little effect on the fatigue life of the SLM specimens subjected to a vertical cyclic load. The number of cycles of the sample subjected to the horizontal cyclic load increases obviously due to preheating. The main reason may be that preheating can inhibit the formation of large size defects.

Conclusions Mechanical properties of the SLM 316L sample have significant anisotropy. The impact absorbing energy of the sample prepared at room temperature is about 47% and 44% of that of the rolled plate, respectively, when the sampling direction is in the horizontal direction and the vertical direction. The tensile strength of the SLM samples prepared at room temperature under a vertical load is about 81.6% of that under a horizontal load. Preheating has little effect on the relative density and impact toughness. Preheating reduces microhardness by about 4%. After preheating, the tensile strength of the 316L sample formed by SLM decreases by about 4% and the elongation increases by about 6%. Under the experimental conditions in this paper, preheating has little effect on the fatigue life of the sample under a vertical load, but significantly improves the fatigue life of the sample under a horizontal load. The main reason may be that preheating can inhibit the formation of large-size defects.

Key words laser technique; selective laser melting; preheating temperature; mechanical property; anisotropy